IEEE Transactions on Automation Science and Engineering (T-ASE) paper presented at
2024 IEEE/RSJ International Conference on Intelligent Robots and Systems (IROS)
October 14-18, 2024. Abu Dhabi, UAE

Safety Compliant, Ergonomic and Time-Optimal Trajectory Planning for Collaborative Robotics

Silvia Proia, *Member, IEEE*, Graziana Cavone, *Senior Member, IEEE*, Paolo Scarabaggio, *Member, IEEE*, Raffaele Carli, *Senior Member, IEEE*, and Mariagrazia Dotoli, *Senior Member, IEEE*

***Abstract*— The demand for safe and ergonomic workplaces is rapidly growing in modern industrial scenarios, especially for companies that intensely rely on Human-Robot Collaboration (HRC). This work focuses on optimizing the trajectory of the end-effector of a cobot arm in a collaborative industrial environment, ensuring the maximization of the operator's safety and ergonomics without sacrificing production efficiency requirements. Hence, a multi-objective optimization strategy for trajectory planning in a safe and ergonomic HRC is defined. This approach aims at finding the best trade-off between the total traversal time of the cobot's end-effector trajectory and ergonomics for the human worker, while respecting in the kinematic constraint of the optimization problem the ISO safety requirements through the well-known Speed and Separation Monitoring (SSM) methodology. Guaranteeing an ergonomic HRC means reducing musculoskeletal disorders linked to risky and highly repetitive activities. The three main phases of the proposed technique are described as follows. First, a manikin designed using a dedicated software is employed to evaluate the Rapid Upper Limb Assessment (RULA) ergonomic index in the working area. Next, a second-order cone programming problem is defined to represent a time-optimal safety compliant trajectory planning problem. Finally, the trajectory that ensures the best compromise between these two opposing goals –minimizing the task's traversal time and maintaining a high level of ergonomics for the human worker– is computed by defining and solving a multi-objective control problem. The method is tested on an experimental case study in reference to an assembly task and the obtained results are discussed, showing the effectiveness of the proposed approach.**

***Note to Practitioners*—Health and safety in workplaces are business imperatives, since they ensure not only a safe collaboration between industrial machinery and human operators, but also an increased productivity and flexibility of the entire industrial process. Hence, investing in health is a real driver for business growth. The key enabling technologies of Industry 4.0, such as collaborative robotics, exoskeletons, virtual and augmented reality, require standardization and indispensable technical safety requirements that cannot ignore physical, sensory, and psychological peculiarities of the human worker and aspects like usability and acceptability of these technologies in performing their activities. Against this ongoing industrial challenge, the aim of this paper is to provide researchers and practitioners with an innovative HRC trajectory planning methodology focused on enhancing production efficiency while respecting the SSM ISO safety requirement and guaranteeing the ergonomic optimal position of the operator during an assembly task. Therefore, the proposed methodology can be a convenient solution to be deployed in industrial companies, since it can support human operators by drastically reducing work-related musculoskeletal disorders and augmenting their performance in the working environment.**

***Index Terms*— Collaborative robotics, human-robot collaboration (HRC), cobots, safety, speed and separation monitoring, ergonomics, rapid upper limb assessment (RULA), time-optimal trajectory planning.**

I. Introduction

HUMAN-ROBOT Collaboration (HRC) is widely recognized as the essential enabling technology of the fourth industrial revolution, also known as Industry 4.0, and as one of the foundation stones of the upcoming Industry 5.0. HRC can improve manufacturing processes, increasing productivity and profitability and, then, leading to prominent positions in the current hyper-competitive industrial scenario.

The goal of the latest collaborative robots, the so-called cobots, is to allow humans and robots to work together in the same industrial environment without compromising the health and safety of workers [1], [2], [3], [4]. In the cobot's design, safety is guaranteed by a large number of proprioceptive and exteroceptive sensors positioned ad hoc to control all movements relative to both internal and external states and by limitations on speed and force that are taken into consideration by the International Standards Organization (ISO) requirements –i.e., Speed and Separation Monitoring (SSM) and Power and Force Limiting (PFL). In the industrial setting, physical and cognitive ergonomics are additional crucial factors to be considered in order to prevent injuries, associated with highly repetitive and dangerous tasks, and to minimize mental stress and psychological discomfort, which could be experienced by operators sharing their working space with cobots.

The implementation of comprehensive analyses to evaluate risk factors for human operators and the development of

Manuscript received 30 November 2022; revised 10 June 2023 and 20 September 2023; accepted 6 November 2023. This article was recommended for publication by Editor M. Zhou upon evaluation of the reviewers' comments. This work was supported in part by the Cognitive Diagnostics Public-Private Laboratory between the Polytechnic University of Bari and Comau S.p.A. Company; and in part by the National Recovery and Resilience Plan (NRRP), Mission 4 Component 2 Investment 1.3—Call for Tender No. 341 of March 2022 of Italian Ministry of University and Research (funded by the European Union—NextGenerationEU) under the Project Circular and Sustainable Made-in-Italy (MICS) under Project PE00000004. *(Corresponding author: Silvia Proia.)*

Silvia Proia, Paolo Scarabaggio, Raffaele Carli, and Mariagrazia Dotoli are with the Department of Electrical and Information Engineering, Polytechnic of Bari, 70125 Bari, Italy (e-mail: silvia.proia@poliba.it; paolo.scarabaggio@poliba.it; raffaele.carli@poliba.it; mariagrazia.dotoli@poliba.it).

Graziana Cavone is with the Department of Civil, Computer Science, and Aeronautical Technologies Engineering, Roma Tre University, 00156 Roma, Italy (e-mail: graziana.cavone@uniroma3.it).

Color versions of one or more figures in this article are available at https://doi.org/10.1109/TASE.2023.3331505.

Digital Object Identifier 10.1109/TASE.2023.3331505

consequent risk reduction strategies are nowadays necessary, due to the rapid increase of work-related musculoskeletal disorders, which are affecting approximately 50% of human workers in industrialized countries. As an example, the HRC designs can incorporate the evaluation of the well-known RULA (Rapid Upper Limb Assessment) [5], [6] and REBA (Rapid Entire Body Assessment) [7] indices to determine the exposure of employees to ergonomic risk factors.

A key factor for an efficient and ergonomic HRC is the development of a systematic procedure that allows the simultaneous optimization of the human worker's well-being and industrial process productivity. Therefore, the aim of this work is to deal with the three pivotal goals of the trajectory planning for a cobot arm in a manufacturing environment, i.e., safety, ergonomics, and efficiency [8], [9]. In particular, the objective is to ensure the best compromise between the traversal time of the trajectory for the cobot and ergonomics for the human worker, while guaranteeing the SSM ISO safety requirement.

The remainder of this paper is structured as follows. Section II sheds light on the main contributions of this work, positioning them with respect to the related literature. Section III delineates the structure of the optimization problem, and in particular the procedure for evaluating the operator's ergonomic posture (Section III-A), the speed and separation monitoring requirement (Section III-B), and the time-optimal trajectory planning along a predefined path while ensuring ISO safety requirements (Section III-C), and the mathematical formulation of the multi-objective optimization (MOO) approach (Section III-D). The case study with the experimental setup and results are discussed in Section IV. Finally, concluding remarks and future developments are reported in Section V.

II. State of the Art and Contribution

Despite the growing amount of papers on HRC, comprehensive literature reviews on the related feedback control problems [9], [21], [22] highlight that only a small percentage of works aims at simultaneously optimizing multiple control targets, such as time, energy, and efficiency. Furthermore, to the best of the authors' knowledge, all scientific contributions addressing the trajectory planning problem for collaborative robots do not aim at simultaneously fulfilling time, safety, and ergonomics requirements, as summarized in Table I. Therefore, the goal and innovation of this work is to develop a novel approach to fill this gap in the HRC control field.

In the scientific and industrial sectors the trajectory planning of robot arms is a well-known and largely discussed topic. Due to the advantages it provides, as well as its issues with the simultaneous optimization of the time interval required to complete the task and of the smoothness of the trajectory execution by the manipulator, time-optimal trajectory planning emerges as an ongoing and complicated research challenge [10]. From the analysis of the related works in the literature, it emerges that the problem of planning a time-optimal motion along a predefined path is mainly performed for traditional industrial robots (see Table I). The time-optimal trajectory planning is eventually extended to a multi-objective optimization problem by combining time and energy optimization.

TABLE I
Summary of Works Related to the Trajectory Planning Optimization Problem

Publication	Optimization target	Resolution method
Industrial robot applications		
[10]	time	direct transcription
[11]	time	indirect
[12]	time	indirect
[13]	time	dynamic programming
[14]	time	dynamic programming
[15]	time	direct transcription
[16]	time	direct transcription
[17]	time	direct transcription
[18]	time-energy	direct transcription
Cobot applications		
[19]	time-safety	direct transcription
[20]	safety-ergonomics	not specified
proposed approach	time-safety-ergonomics	direct transcription

Still, the majority of works are related to industrial robots, whose main aim is to remove humans from hazardous, hard and dirty jobs in industry. In this context, the available contributions can be classified into three categories, based on the programming methodology used to solve the optimization problem, i.e., indirect methods, dynamic programming methods, and direct transcription methods (see Table I - column III). The indirect methods [11], [12] are more precise than the other two methods, but they are difficult to implement, since they find the numerical solution through a procedure based on "forward" and "backward" integrations and require the implementation of a certain number of steps, which need the choice of tolerance and stop criteria. An alternative approach is represented by dynamic programming methods [13], [14], based on the principle of the mathematician Richard Bellman, that simplifies a trajectory planning problem by decomposing it into simpler sub-problems in a recursive manner. The third category consists of the direct transcription methods, used in [10], [15], [16], [17], [18], [19], that are even less precise, but are easier to implement, being based on the resolution of non linear systems, which can be solved by ad hoc "solvers" that compute the solution to the problem in a short time and efficiently.

Only recently, due to the advances in industrial automation introduced by the Industry 4.0 key enabling technologies [23], [24], the scientific community has focused on collaborative robotics and dedicated efforts to the related trajectory planning problem. However, although time and safety are critical HRC requirements, to the best of our knowledge, only one work [19] proposes a trajectory planning algorithm to plan fast and safe motions for cobots. In particular, in [19], the time-optimal planning is combined with a safety evaluation module for collaborative robots in shared environments.

Finally, also ergonomics is barely considered in HRC control targets. Indeed, one of the few works considering safety and ergonomics but not time for industrial co-manipulators is the article [20] by Ferraguti et al., as the control architecture incorporates two working modes, an ergonomic planner and an admittance controller that can be initialized in a mutually exclusive manner.

With the aim of filling the discussed gaps, this paper, which comes as an extension of the article [25], proposes a novel methodology for the trajectory planning of a cobot arm that aims at simultaneously optimizing time and ergonomics, while guaranteeing safety for the human worker through the SSM ISO requirement. First, we propose a time-optimal trajectory planning problem that integrates the SSM safety requirements in accordance with the ISO/TS 15066 standards [26]. Unlike our previous work [25], the proposed approach integrates the SSM into the kinematic constraint of the optimization problem, limiting the speed of the robot's end-effector. This innovation, along with the technical limits on joint speed and acceleration described in [25], allows reducing the risk of injury as specified in the ISO technical specification for collaborative robots. Consequently, our approach enhances the overall operator safety and improves the capabilities of the control system. The time-optimal trajectory planning task is then solved using a direct transcription method, transforming the initial non linear and non convex optimal control problem into a convex optimization problem in Second-Order Cone Programming (SOCP) form [17]. This ensures the existence and uniqueness of a solution to the problem. Additionally, to ensure ergonomic collaboration, reduce operator fatigue, increase comfort, and boost productivity, we define a systematic procedure for evaluating the RULA index in the whole collaborative working space [5], [6]. Finally, by solving a multi-objective control problem, we determine a trajectory that strikes the best balance between minimizing task traversal time and maintaining a high level of ergonomics for the human operator. Differently from [25], we perform a sensitivity analysis to assess the uncertainty associated with the non-optimal positioning of the cobot's end-effector, using the results obtained from the Multi-Objective Optimization (MOO) problem. We remark that, to the best of our knowledge, there is no paper in the literature that simultaneously addresses the trajectory planning problem considering efficiency and safety while also ensuring a comfortable and ergonomic working environment for human operators.

The method proposed in this work has a number of potential applications in the context of Industry 4.0. In particular, the approach can be employed in tasks where high precision is needed, ranging from pick and place to accurate assembly (e.g., screw driving, nut driving, part fitting), material removal, or any other specific application that can be associated with the "3D" (Dull, Dirty, Dangerous). An experimental case study is analyzed to verify the effectiveness of the suggested approach in one of the aforementioned industrial scenarios.

III. The Proposed Methodology

The main objective of this work is to ergonomically optimize the posture for the operator and satisfy the SSM ISO safety requirement during the trajectory planning of the task to be performed by the cobot in the shortest possible time.

In particular, the considered industrial scenario examines the collaboration in a shared workspace between a human operator and a cobot that moves with its end-effector a workpiece on which the human is expected to complete some operations. All the tasks performed by the cobot must take into account the safety of the human operator. The cobot follows a trajectory that minimizes the time required to move the object from a fixed starting point to an end point that is ergonomically optimal for the operator, with the aim of reducing the musculoskeletal disorders that may arise, especially in highly repetitive tasks.

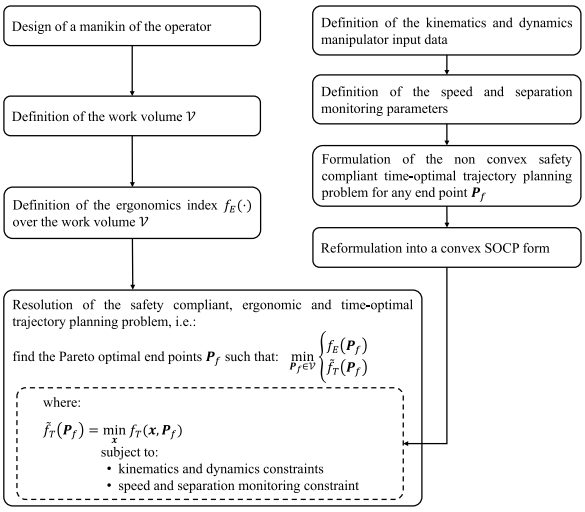

Fig. 1. Overview diagram of the proposed methodology.

Figure 1 summarizes all the steps of the proposed methodology. The formulation of the multi-objective control problem (bottom of the diagram) – aimed at finding the best compromise between the ergonomics for the human worker and the traversal time of the trajectory for the cobot, while guaranteeing the SSM ISO safety requirement inside the kinematic constraint (see Section III-D) and thus, at allowing the offline solution of the trajectory planning problem – relies on some preliminary steps related to the evaluation of ergonomics, and to the formulation of the time-optimal safety compliant trajectory planning along a predefined path. On the one hand, a three-step systematic procedure (described in the three blocks on the top-left of the diagram) is conducted with the aim of determining the level of ergonomics in terms of RULA index (denoted as $\boldsymbol{f}_E(\boldsymbol{P}_f)$ as detailed in the sequel) for a set of potential end points (denoted as $\boldsymbol{P}_f$ as detailed in the sequel) of the planned cobot's trajectory (see Section III-A). On the other hand, for any end point, the time-optimal safety compliant trajectory planning problem is converted into a SOCP problem following the steps illustrated in the top-right of the diagram. The first preliminary step consists in generating the path and defining the kinematics and dynamics manipulator input data, i.e., the starting and ending pose, the Denavit-Hartenberg parameters, and the kinematic and dynamics indicators. In the second step, the speed and separation monitoring parameters (see Section III-B) are defined in order to be included in the kinematic constraint. Then, the non convex time-optimal safety compliant trajectory planning problem is formulated by defining the objective function and the kinematic and dynamic constraints. Finally, by performing the convex relaxation, such problem is discretized and transformed into a convex optimization problem in SOCP form (see Section III-C), whose resolution consists in optimizing one of the objective functions (denoted as $\tilde{f}_T(\boldsymbol{P}_f)$ as detailed in the

sequel) of the MOO problem (dashed block at the bottom of the diagram).

A. Evaluation of Ergonomics in HRC

In this section, we present the specific procedure to determine the ergonomics' level. This novel procedure is based on three steps and employs the Rapid Upper Limb Assessment (RULA) index to classify the set of potential end points of the planned cobot's trajectory.

Different criteria, including the RULA, Rapid Entire Body Assessment (REBA), postural Loading on the Upper Body Assessment (LUBA), and Occupational Repetitive Action (OCRA), are nowadays employed in the related literature to estimate the ergonomics of a given posture [27]. We employ the RULA index as a means of assessing the ergonomic posture of the operator as we are interested in reducing upper limb disorders in the investigated industrial setting. Nevertheless, the procedure described in the sequel is still valid replacing the RULA with other evaluation indicators.

The RULA index is calculated by analyzing postures, repetitiveness of movements, applied strength, and static musculoskeletal activity. To this aim, each of the main body areas -arm, forearm, wrist, neck, and trunk- receives a score. Each RULA score corresponds to a degree of risk exposure ranging from 0 (representing a minimal risk requiring no special countermeasure) to 6 (corresponding to high risk). Note that one RULA test can only measure the effort made by the right or left side of the body.

Ad hoc computer-aided design and engineering software, such as CATIA [28] or Process Simulate (Siemens) [29], can be used to evaluate ergonomics of human operators in generic workspaces. With the help of these tools, it is possible to easily design virtual manikins that represent the operator and consequently simulate any possible working condition in a given work volume.

The first step of the proposed systematic procedure is therefore the design of a virtual manikin in the selected tool to assess the operator's ergonomic posture. During this phase, a number of different features can be given in the manikin configuration, such as gender, percentile applied to the stature (height), weight, and any other anthropometric factors determined in accordance with the selected reference population. Note that during the characterization of the manikin it is convenient to place its initial reference point between its feet.

The second step of the procedure is the definition of a work volume $\mathcal{V} \subseteq \mathbb{R}^3$, whose dimensions depend on the characteristics of the manikin generated in the previous phase. The work volume is made of a set of points $\boldsymbol{P}_f \in \mathcal{V}$ that the manikin arm is able to reach and that coincides with all the endpoints of the trajectory that the end-effector can follow.

Then, in the third step of the procedure the ergonomics function $f_E(\boldsymbol{P}_f)$, i.e., the function that estimates ergonomics in terms of RULA for each candidate point $\boldsymbol{P}_f \in \mathcal{V}$, is determined with a Design of Experiments (DOE). For each candidate point, the RULA is estimated considering that the manikin simulates an operator standing and handling a tool in a posture that allows to reach the candidate point.

As previously mentioned, the RULA index allows the evaluation of the ergonomic posture with regard to just one side of the body. Hence, for a right-handed person, the RULA analysis must be carried out on the right side, and for a left-handed person, on the left side. It is important to note that the previously defined work volume will be mirrored around the mid-sagittal plane of the body for a left-handed person. Additionally, the frequency at which the operation is performed as well as the load of the manipulated item must be specified during the evaluation of the RULA index. It is evident that the RULA score grows when task repetition and load increase.

B. Speed and Separation Monitoring Requirement

HRC is leaving behind the traditional paradigm of robots living in separate safety cages, allowing human operators to work side-by-side with "fenceless" robots for completing an increasing number of complex industrial tasks. Consequently, the safety of human operators is nowadays understood as a fundamental requirement in collaborative robotic applications.

In the related literature, several control algorithms have been implemented to safely guide a robot during the execution of its tasks. These approaches avoid dangerous situations by defining safety regions, that the robot cannot access, or by dynamically tracking the separation distance between the robot and other obstacles, such as human operators [9].

According to the ISO/TS 15066 standards, safety can be guaranteed by limiting the maximum permissible forces or torques and consequently the energy transfer on potential direct physical contact between the operator and the robot, i.e., PFL, or by prescribing that the speed must be related to a certain separation distance between the human and the robot, i.e., SSM. In the current work, we assume that no undesired contact must happen between the operator and the cobot arm. Thus, during the collaboration, the SSM ISO safety requirement is chosen to help safeguard the operator by allowing the robot actuation system to have the deceleration capability necessary to achieve a complete stop before eventually coming in contact with the operator [30], [31].

With the aim of preserving a safe separation distance between the operator and the cobot arm, the SSM method monitors the regions surrounding the robot, and issues a command to slow or stop the robot as the human operator approaches. This method is based on the continuous measurement of the distance between the robot and a detected operator (i.e., the human-robot separation distance), which is compared with the so-called authorized (operator protective) distance [32], [33]. Hence, when the separation distance is lower than the authorized distance, and consequently when the cobot arm enters the collaborative working zone (Fig. 2a), the SSM system decreases the robot's speed, initiating a safety-rated controlled stop to avoid an impact with the operator (Fig. 2b). The robot may then resume its motion once the separation distance is greater than the authorized distance.

More in detail, the minimum allowable human-robot distance S at a given time t_0 is computed by using the equation prescribed in ISO/TS 15066 [26], that is:

$$S(t_0) = S_h + S_r + S_s + C + Z_d + Z_r \tag{1}$$

where S_h and S_r indicate the operator's and robot's change in location, respectively, and S_s is the maximum stopping

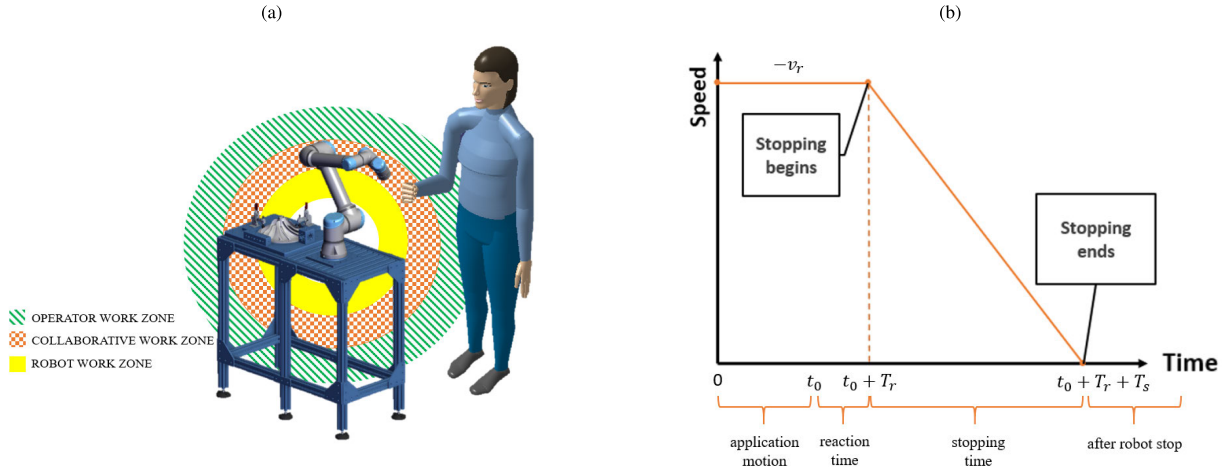

Fig. 2. Scheme of the SSM criterion with the operator (green), collaborative (orange), and robot (yellow) working zones (a). Profile of the robot speed during the task execution (b).

distance of the robot. The remaining terms of (1) capture the uncertainty of measurements, being C an intrusion distance safety margin based on the expected human reach and $Z_d + Z_r$ the position uncertainty for both the robot and operator.

Equation (1) can be reformulated under static conditions, i.e., assuming a constant speed of the robot, as follows:

$$S(t_0) = (v_h(t_0)T_r + v_h(t_0)T_s) + v_r T_r + B + C + Z_d + Z_r \tag{2}$$

where $v_h(t_0)$ indicates the speed of the operator (i.e., the rate of the operator's motion toward the robot), v_r is the speed of the robot directed towards the operator in the collaborative work zone, T_r represents the time for the robot system to respond to the operator's presence, including the time required to detect the position of the operator, process this signal, and activate the robot's stop, and finally T_s is the time to safely stop the motion of the robot. Note that T_s is a function of the robotic system configuration, planned movement, speed, and load, while parameter B denotes the braking distance traveled by the cobot arm.

In particular, since in our work the operator is in a fixed standing position, v_h is equal to zero as well as parameter C and uncertainties $Z_d + Z_r$. Hence, given our assumptions, (2) may be rewritten as:

$$S(t_0) = v_r T_r + B \tag{3}$$

where parameter B is computed as $v_r^2/2a_r$ with a_r being the worst-case deceleration value of the robot during the stopping procedure. In Fig. 2b, we report the profile of the robot's speed v_r as a function of time, which drops abruptly once the robot enters into the collaborative work zone.

With the aim of controlling the robot's speed, the SSM criterion is applied in the kinematic constraint of the time-optimal safety compliant trajectory planning along a predefined path problem (see Section III-C). In particular, being the human-robot distance $S(t_0)$ known at each given time, in (3) the allowed speed v_r is treated as an unknown. From the resolution of the second degree equation (3) with respect to v_r we get two speed values, one of which is positive and one negative. Among these two solutions, we disregard the negative one having no physical meaning while we employ the positive speed value $\overline{v}_r$ as the upper limit of the kinematic constraint as follows:

$$v_r \leq \overline{v}_r. \tag{4}$$

C. Time-Optimal Safety Compliant Trajectory Planning Along a Predefined Path

In this section we formulate the problem of planning the trajectory of the cobot, aiming at minimizing the traversal time, from a fixed starting point $\boldsymbol{P}_i \in \mathbb{R}^3$ to a given ergonomically optimal end point $\boldsymbol{P}_f \in \mathcal{V} \subseteq \mathbb{R}^3$. We specifically assume that the end-effector of the cobot must follow a geometrical rectilinear path between these two points while satisfying the SSM requirement inside the kinematic constraint and the imposed kinematic and dynamic joint's limits.

Without loss of generality, we assume that the trajectory starts at time $t = 0$ in $\boldsymbol{P}_i$ and ends at time $t = T$ in $\boldsymbol{P}_f$. Hence, by defining the time-dependent scalar path coordinate $s(t)$, we have that $s(0) = 0 \leq s(t) \leq 1 = s(T)$. For the sake of notation clarity, we omit the time dependency of s and its derivatives in the rest of this manuscript.

As the aforementioned geometric path is given in the operational spatial coordinates, let us employ the kinematic inversion to obtain the path in joint space coordinates. More in detail, we consider a generic n-DOF (degree of freedom) robotic manipulator, that can be represented by its configuration, i.e., the angular position of its n joints $\boldsymbol{q} \in \mathbb{R}^n$. The goal of the inverse kinematic is therefore to define a map that, given the scalar time dependent path coordinate $s(t)$, calculates the related path in joint space coordinates $\boldsymbol{q}(s) \in \mathbb{R}^n$.

By following the procedures outlined in [18], the joint velocities and accelerations for the given path $\boldsymbol{q}(s)$ can be expressed using the chain rule as follows:

$$\dot{\boldsymbol{q}} = \boldsymbol{q}'(s)\dot{s} \tag{5}$$

$$\ddot{\boldsymbol{q}} = \boldsymbol{q}'(s)\ddot{s} + \boldsymbol{q}''(s)\dot{s}^2 \tag{6}$$

where $\boldsymbol{q}'(s) = \frac{\delta \boldsymbol{q}(s)}{\delta s}$ and $\boldsymbol{q}''(s) = \frac{\delta^2 \boldsymbol{q}(s)}{\delta^2 s}$ represent the first and second partial derivatives of the geometric path $\boldsymbol{q}(s)$ with respect to parameter s, whereas $\dot{s} = \frac{\delta s}{\delta t}$ and $\ddot{s} = \frac{\delta^2 s}{\delta^2 t}$ represent

the pseudo-speed and pseudo-acceleration along the path, respectively. We remark that s is a monotonically increasing parameter, and thus it holds $\dot{s} > 0$.

Let us express the dynamical equation of motion for the robotic manipulator as a function of the applied torques $\boldsymbol{\tau} \in \mathbb{R}^n$ in each joint:

$$\boldsymbol{M}(\boldsymbol{q})\ddot{\boldsymbol{q}} + \boldsymbol{C}(\boldsymbol{q}, \dot{\boldsymbol{q}})\dot{\boldsymbol{q}} + \boldsymbol{F}_v\dot{\boldsymbol{q}} + \boldsymbol{F}_s \operatorname{sgn}(\dot{\boldsymbol{q}}) + \boldsymbol{g}(\boldsymbol{q}) = \boldsymbol{\tau} \tag{7}$$

where we define $\boldsymbol{M}(\boldsymbol{q}) \in \mathbb{R}^{n\times n}$ as a positive definite mass matrix, $\boldsymbol{C}(\boldsymbol{q}, \dot{\boldsymbol{q}}) \in \mathbb{R}^{n\times n}$ as a matrix taking into account the Coriolis and centrifugal factors, $\boldsymbol{g}(\boldsymbol{q}) \in \mathbb{R}^n$ as the vector denoting the gravitational torques, and lastly $\boldsymbol{F}_v, \boldsymbol{F}_s \in \mathbb{R}^{n\times n}$ as diagonal matrices that represent the coefficients of viscous and Coulomb friction, respectively.

By replacing (5) and (6) in (7), and neglecting the impact of viscous and Coulomb frictions $\boldsymbol{F}_v\dot{\boldsymbol{q}} + \boldsymbol{F}_s \operatorname{sgn}(\dot{\boldsymbol{q}})$, we obtain the following dynamic equation:

$$\boldsymbol{a}_1(s)a(s) + \boldsymbol{a}_2(s)b(s) + \boldsymbol{a}_3(s) = \boldsymbol{\tau}(s) \tag{8}$$

where $\boldsymbol{a}_i(s) \in \mathbb{R}^n, i = 1, 2, 3$ are defined as:

$$\boldsymbol{a}_1(s) = \boldsymbol{M}(\boldsymbol{q}(s))\boldsymbol{q}'(s) \tag{9}$$

$$\boldsymbol{a}_2(s) = \boldsymbol{M}(\boldsymbol{q}(s))\boldsymbol{q}''(s) + \boldsymbol{C}(\boldsymbol{q}(s), \boldsymbol{q}'(s))\boldsymbol{q}'(s) \tag{10}$$

$$\boldsymbol{a}_3(s) = \boldsymbol{g}(\boldsymbol{q}(s)) \tag{11}$$

and:

$$a(s) = \ddot{s} \tag{12}$$

$$b(s) = \dot{s}^2 \tag{13}$$

are optimization variables introduced to allow a convexification of the trajectory planning problem [17]. Furthermore, to solve the time-optimal trajectory planning problem, the following linear differential equality constraint must be included:

$$b'(s) = 2a(s) \tag{14}$$

which follows from the fact that:

$$\dot{b}(s) = b'(s)\dot{s} = 2\dot{s}\ddot{s} \leftrightarrow b'(s) = 2a(s) \;\text{ if }\; \dot{s} > 0. \tag{15}$$

Having defined the dynamical equations of the manipulator, let us now represent a number of technical constraints that must be included in the trajectory planning problem.

First, we include the torque limit constraints as follows:

$$\underline{\boldsymbol{\tau}}(s) \le \boldsymbol{\tau}(s) \le \overline{\boldsymbol{\tau}}(s) \tag{16}$$

where we define $\underline{\boldsymbol{\tau}}(s) \in \mathbb{R}^n$ and $\overline{\boldsymbol{\tau}}(s) \in \mathbb{R}^n$, with $\underline{\boldsymbol{\tau}}(s) = -\overline{\boldsymbol{\tau}}(s)$, as the lower and upper limits on joints torques that are a function of s. Note that (16) is necessary to obtain a solution for the trajectory planning problem that guarantees a positive traversal time, i.e., $T > 0$.

In addition to the above constraints on torques, let us now describe in detail the constraints on the kinematic variables. These constraints must be included in order to satisfy the technical limitations imposed by the HRC task and to guarantee the SSM requirements and thus, safety of the human operator.

On the one hand, the speed limits are defined as:

$$\underline{\dot{\boldsymbol{q}}}(s) \le \dot{\boldsymbol{q}}(s) \le \overline{\dot{\boldsymbol{q}}}(s) \tag{17}$$

where $\underline{\dot{\boldsymbol{q}}}(s) \in \mathbb{R}^n$ and $\overline{\dot{\boldsymbol{q}}}(s) \in \mathbb{R}^n$, with $\underline{\dot{\boldsymbol{q}}}(s) = -\overline{\dot{\boldsymbol{q}}}(s)$, are the lower and upper limits of the robot's speed. More specifically, $\underline{\dot{q}}_i(s)$ and $\overline{\dot{q}}_i(s)$ with $i = 1, \ldots, n-1$ represent the technical limits of the robot's joints, whereas $\underline{\dot{q}}_n(s)$ and $\overline{\dot{q}}_n(s)$ represent the limits of the robot's end-effector. In particular, $\overline{\dot{q}}_n(s)$ is set equal to $\overline{v}_r$ in compliance with the SSM ISO safety requirement for the operator (i.e., inequality (4)). Note that the SSM criterion is applied to limit the speed of the robot's end-effector which will then affect the slowdown of the entire kinematic chain. Inequality (17) can be conveniently reformulated as:

$$(\boldsymbol{q}'(s) \odot \boldsymbol{q}'(s))b(s) \le \overline{\dot{\boldsymbol{q}}}^2(s) \tag{18}$$

due to the fact that $\underline{\dot{\boldsymbol{q}}}(s) \le \dot{\boldsymbol{q}}(s) \le \overline{\dot{\boldsymbol{q}}}(s) \leftrightarrow \dot{\boldsymbol{q}}(s)^2 = (\boldsymbol{q}'(s)\dot{s})^2 = (\boldsymbol{q}'(s) \odot \boldsymbol{q}'(s))b(s) \le \overline{\dot{\boldsymbol{q}}}^2(s)$.

On the other hand, the acceleration limits are:

$$\underline{\ddot{\boldsymbol{q}}}(s) \le \ddot{\boldsymbol{q}}(s) \le \overline{\ddot{\boldsymbol{q}}}(s) \tag{19}$$

where $\underline{\ddot{\boldsymbol{q}}}(s) \in \mathbb{R}^n$ and $\overline{\ddot{\boldsymbol{q}}}(s) \in \mathbb{R}^n$, with $\underline{\ddot{\boldsymbol{q}}}(s) = -\overline{\ddot{\boldsymbol{q}}}(s)$, represent the lower and upper limits of the acceleration, respectively. Similarly to the velocity, also in this case we can rewrite (19) as:

$$\underline{\ddot{\boldsymbol{q}}}(s) \le \boldsymbol{q}''(s)b(s) + \boldsymbol{q}'(s)a(s) \le \overline{\ddot{\boldsymbol{q}}}(s). \tag{20}$$

Clearly, by adding the limits on speed and acceleration, the total traversal time T will not be the optimal one, but rather a compromise between safety for the human operator and efficiency of the task.

By changing the integration variable from t to s after completing the aforementioned preceding stages, it is straightforward to formulate the objective function of the time-optimal trajectory planning problem. The goal is to minimize the total traversal time, defined as:

$$T = \int_0^T dt = \int_0^1 \left(\frac{ds}{dt}\right)^{-1} ds = \int_0^1 \frac{1}{\dot{s}} ds. \tag{21}$$

In addition, by defining:

$$c(s) = \sqrt{b(s)} = \dot{s} \tag{22}$$

and since $b(s), c(s) \ge 0$ during the trajectory, we can rewrite the objective function (21) as follows:

$$T = \int_0^1 \frac{1}{\dot{s}} ds = \int_0^1 \frac{1}{\sqrt{b(s)}} ds = \int_0^1 \frac{1}{c(s)} ds. \tag{23}$$

Note that the integral in (23) is defined in the interval $[0^+, 1^-]$, as the objective function has no upper bound when the initial and final pseudo-speeds are zero.

Summing up, let us formulate the time-optimal trajectory planning problem as:

$$\begin{aligned}
\underset{a(s),b(s),c(s),\boldsymbol{\tau}(s)}{\text{minimize}} \quad & \int_{0^+}^{1^-} \frac{1}{c(s)} ds \\
\text{subject to} \quad & b(0) = \dot{s}_0{}^2, b(1) = \dot{s}_T{}^2 \\
& c(0) = \dot{s}_0, c(1) = \dot{s}_T \\
& \boldsymbol{\tau}(s) = \boldsymbol{a}_1(s)a(s) + \boldsymbol{a}_2(s)b(s) + \boldsymbol{a}_3(s) \\
& \underline{\boldsymbol{\tau}} \le \boldsymbol{\tau}(s) \le \overline{\boldsymbol{\tau}}
\end{aligned}$$

$$
\begin{aligned}
&\forall s \in [0,1]\\
&b'(s) = 2a(s)\\
&c(s) = \sqrt{b(s)}\\
&(\boldsymbol{q}'(s) \odot \boldsymbol{q}'(s))b(s) \le \bar{\dot{\boldsymbol{q}}}^{2}(s)\\
&\underline{\ddot{\boldsymbol{q}}}(s) \le \boldsymbol{q}''(s)b(s) + \boldsymbol{q}'(s)a(s) \le \bar{\ddot{\boldsymbol{q}}}(s)\\
&b(s), c(s) \ge 0\\
&\forall s \in [0^+, 1^-].
\end{aligned} \tag{24}
$$

Let us gather the decision variables in one decision vector:

$$
\boldsymbol{x} = (a(s), b(s), c(s), \boldsymbol{\tau}(s)^\top)^\top \tag{25}
$$

and then, let us rewrite the above problem in a compact form by defining $f_T(\cdot)$ as the function expressing the total traversal time with respect to the end point $\boldsymbol{P}_f$ and trajectory parameters $\boldsymbol{x}$ in (25):

$$
\begin{aligned}
&\underset{\boldsymbol{x}}{\text{minimize}} \quad f_T(\boldsymbol{x}, \boldsymbol{P}_f)\\
&\text{subject to} \quad \text{constraints (24)}.
\end{aligned} \tag{26}
$$

There are a variety of approaches (such as indirect methods, dynamic programming methods, and direct transcription methods) that are commonly used to address problem (26), however, for the sake of simplicity and computational speed, we opted for the methodology suggested by [17]. In particular, we perform the "convex relaxation" by transforming the unique non linear equality constraint $c(s) = \sqrt{b(s)}$ with the equivalent expression $\frac{1}{\sqrt{b(s)}} \le \frac{1}{c(s)}$, and then we convert the optimal control problem (24) into a convex optimization problem in SOCP form using the direct transcription technique and the relation $d(s) \ge \frac{1}{c(s)}$. The resulting convex optimization problem can be solved by one of several tools available for convex programming and is formally defined as follows:

$$
\begin{aligned}
\underset{a_k, b_k, c_k, d_k, \boldsymbol{\tau}_k}{\text{minimize}} \; & \frac{1}{2}[(1-\alpha)\Delta s_1 (d(0^+) + d_2)\\
& + \sum_{k=2}^{N-2} \Delta s_k (d_k + d_{k+1})\\
& + (1-\alpha)\Delta s_{N-1}(d_{N-1} + d(1^-))]\\
\text{subject to} \quad & b_1 = \dot{s}_0^{\,2}, \; b_N = \dot{s}_T^{\,2}\\
& c_1 = \dot{s}_0, \; c_N = \dot{s}_T\\
& \boldsymbol{\tau}_k = \boldsymbol{a}_1(s_k)a_k + \boldsymbol{a}_2(s_k)b_k + \boldsymbol{a}_3(s_k)\\
& \underline{\boldsymbol{\tau}} \le \boldsymbol{\tau}(s_k) \le \bar{\boldsymbol{\tau}}\\
& \left\| \begin{bmatrix} 2c_k \\ b_k - 1 \end{bmatrix} \right\|_2 \le b_k + 1\\
& (\boldsymbol{q}'(s_k) \odot \boldsymbol{q}'(s_k))b(s_k) \le \bar{\dot{\boldsymbol{q}}}^{2}(s_k)\\
& \underline{\ddot{\boldsymbol{q}}}(s_k) \le \boldsymbol{q}''(s_k)b(s_k) + \boldsymbol{q}'(s_k)a(s_k) \le \bar{\ddot{\boldsymbol{q}}}(s_k)\\
& \quad \text{for } k = 1, \ldots, N\\
& b_{j+1} - b_j = \Delta s_j (a_{j+1} + a_j)\\
& \text{for } j = 1, \ldots, N-1\\
& b_l > 0, \;\; c_l > 0\\
& \left\| \begin{bmatrix} 2 \\ c_l - d_l \end{bmatrix} \right\|_2 \le c_l + d_l \quad \text{for } l = 2, \ldots, N-1\\
& \left\| \begin{bmatrix} 2 \\ c(0^+) - d(0^+) \end{bmatrix} \right\|_2 \le c(0^+) + d(0^+)\\
& \left\| \begin{bmatrix} 2 \\ c(1^-) - d(1^-) \end{bmatrix} \right\|_2 \le c(1^-) + d(1^-)
\end{aligned} \tag{27}
$$

where parameter $\Delta s_j = s_{j+1} - s_j$, $j = 1, 2, \ldots, N-1$ is a discretization interval while $\alpha > 0$ is a technical parameter that can be adjusted based on the applicative scenario. The solution of problem (27), i.e., $a^*(s), b^*(s), c^*(s), d^*(s)$, and $\boldsymbol{\tau}^*(s)$, is computed at the sampling points $s_1 = 0 < s_2 < \ldots < s_N = 1$. Clearly, it is possible to derive $\boldsymbol{q}_d^*(t), \dot{\boldsymbol{q}}_d^*(t), \ddot{\boldsymbol{q}}_d^*(t)$, and $\boldsymbol{\tau}_d^*(t)$ as we remark that a one-to-one correspondence between s and t is enforced. Hence, the last step is to compute time t with the inverse relation shown below:

$$
t(s) = t(0^+) + \int_{0^+}^{s} \frac{1}{c(u)} du \tag{28}
$$

that can be expressed as a function of the previously discretized k-th parameter $1/c(s) = d(s)$ as follows:

$$
\begin{aligned}
t(s_k) &= t(s_{k-1}) + \int_{s_{k-1}}^{s_k} d(u) du\\
&= t(s_{k-1}) + \frac{1}{2}\Delta s_{k-1}(d_{k-1} + d_k)
\end{aligned} \tag{29}
$$

for $k = 1, \ldots, N$. The value corresponding to t_N is therefore the total traversal time T of the planned trajectory.

Note that the problem (27) is a convex optimization problem. As, it is well known, convexity in optimization problems guarantees the existence and uniqueness of a solution and ensures the convergence of the solver [34]. The convexity of the trajectory planning problem provides strong theoretical assurances regarding the effectiveness and reliability of our approach. It ensures that the optimization algorithm will converge to an optimal solution that satisfies both the time optimization objective and the safety constraint, further strengthening the practical applicability and effectiveness of our methodology.

D. Formulation of the Multi-Objective Optimization Problem

This section is devoted to the description of the MOO problem that determines the optimal cobot trajectory by seeking a trade-off solution between two different needs. In detail, the MOO approach aims at efficiently operating the robot, that is minimizing the traversal time with the constrained trajectory planning optimal control problem in Section III-C, and maximizing the ergonomics level for the human worker in Section III-A, while respecting the SSM ISO safety requirement in Section III-B.

More in detail, for a given starting point $\boldsymbol{P}_i$, the MOO problem seeks to choose the best end point $\boldsymbol{P}_f \in \mathcal{V}$ such that the corresponding RULA ergonomics index is minimized and the associated trajectory parameters $\boldsymbol{x}$ defined in (25) correspond to a traversal time that can be safely attained by the end-effector of the cobot in the shortest time. The MOO problem can be formally defined as follows:

$$
\min_{\boldsymbol{x}, \boldsymbol{P}_f} \begin{cases} f_E(\boldsymbol{P}_f) \\ f_T(\boldsymbol{x}, \boldsymbol{P}_f) \end{cases}
$$

$$\text{subject to} \quad \text{constraints (24) and} \quad \boldsymbol{P}_f \in \mathcal{V} \tag{30}$$

where we recall that $f_E(\boldsymbol{P}_f)$ indicates the evaluation of the RULA index for the end point $\boldsymbol{P}_f$ varying over the work volume $\mathcal{V}$ while $f_T(\boldsymbol{x}, \boldsymbol{P}_f)$ denotes the total traversal time along the rectilinear path connecting the fixed initial point $\boldsymbol{P}_i$ and the end point $\boldsymbol{P}_f$ given the trajectory parameters $\boldsymbol{x}$.

By leveraging the parametric optimization properties (i.e., $\min_{y,z} f(y,z) = \min_y(\min_z f(y,z)) = \min_y \tilde{f}(y)$ where $\tilde{f}(y) = \min_z f(y,z)$) [34], we can define the parametric optimization function $\tilde{f}_T(\boldsymbol{P}_f)$ as:

$$\begin{aligned} \tilde{f}_T(\boldsymbol{P}_f) = & \min_{\boldsymbol{x}} f_T(\boldsymbol{x}, \boldsymbol{P}_f) \\ & \text{subject to} \\ & \text{constraints (24)} \end{aligned} \tag{31}$$

and thus we can transform the MOO problem (30) in the following equivalent form:

$$\begin{aligned} \min_{\boldsymbol{P}_f} & \begin{cases} f_E(\boldsymbol{P}_f) \\ \tilde{f}_T(\boldsymbol{P}_f) \end{cases} \\ \text{subject to} \quad & \boldsymbol{P}_f \in \mathcal{V}. \end{aligned} \tag{32}$$

The MOO problem in (32) has, in general, a number of (possibly infinite) solutions. Nevertheless, there may not exist a single solution that simultaneously optimizes the two above-mentioned objectives, which are therefore said to be conflicting. Informally speaking, a solution for the MOO problem in (32) is called Pareto optimal if none of the two conflicting objectives functions, i.e., $\tilde{f}_T$ and f_E, can be improved without degrading the other one. Hence, we can identify different Pareto optimal points $\boldsymbol{P}_f \in \mathcal{V}$, corresponding to solutions with minimum RULA index, shorter traversal time, and intermediate trade-offs between time and ergonomics. The choice of the final solution for (32) depends on the prioritization given by the HRC targets, in fact, without additional preferences, all the Pareto optimal solutions are considered equally good [35], [36], [37], [38].

IV. Case Study

A. Experimental Setup

In this section we describe the experimental setup of the proposed MOO trajectory planning approach for a safe and ergonomic HRC. The goal of our case study is to safely and ergonomically perform an assembly task in an industrial scenario where an operator works closely with a cobot. In detail, we assume that a cam organ is moved and oriented by the cobot's end-effector in such a way as to allow its assembly inside the engine head where the operator inserts the screws as efficiently and ergonomically as possible (Fig. 3).

All the experiments are conducted on a laptop with a 2.5 GHz Intel Core i5-7200U CPU and 8 GB RAM using the CAD software CATIA V5 [28] and MATLAB.

The main focus is the time optimization along the desired trajectory followed by the cobot from a fixed starting point $\boldsymbol{P}_i = (P_{x_i}, P_{y_i}, P_{z_i})^\top = (0.6, -0.1, 1.7)^\top$ (coordinates in meters) to an ergonomically optimal end point

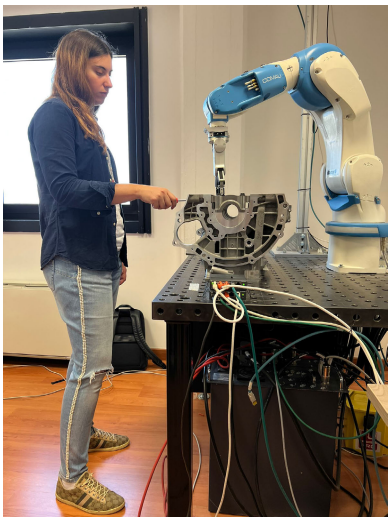

Fig. 3. The assembly task performed in a safe and ergonomic HRC.

$\boldsymbol{P}_f = (P_{x_f}, P_{y_f}, P_{z_f})^\top$ for the operator. The end points should be comprised in the work volume $\mathcal{V}$, comprehending all candidate points where the cobots and the operator may interact, that is designed as a rectangular cuboid with the subsequent bounding dimensions (in meters): $P_{x_f,min} = 0.2$, $P_{x_f,max} = 0.5$, $P_{y_f,min} = -0.5$, $P_{y_f,max} = 0.1$, $P_{z_f,min} = 1$, $P_{z_f,max} = 1.5$.

In order to perform the collaborative assembly, we design a human operator on the CAD software CATIA. In particular, we consider a real right-handed female operator with height and weight percentile equal to 95 and 80, respectively. The initial referential point of the manikin is chosen between the feet for the evaluation of the operator's ergonomic posture.

Subsequently, a DOE is performed in order to identify the ergonomics function $f_E(\boldsymbol{P}_f)$, i.e., the function that quantifies ergonomics in terms of RULA for each candidate point $\boldsymbol{P}_f \in \mathcal{V}$. To this aim, we divide the given work volume $\mathcal{V}$ into u rectangular cuboids $\mathcal{V}_u \subseteq \mathcal{V}$ of equal size and we assume that the ergonomics function is constant within these volumes. i.e., $f_E(\boldsymbol{P}_f)$ is constant for all $\boldsymbol{P}_f \in \mathcal{V}_u$. Note that this assumption allows fast identification of the ergonomics function and, for a sufficiently high number of cuboids, also an accurate computation of ergonomics for each candidate point. For the presented scenario we assume a number of cuboids equal to $u = 225$ with sizes (in meters) of 0.06, 0.12 and 0.05 along the X, Y, and Z axis, respectively. Then, we compute the RULA index for the centroid C_u of each of these cuboids $\mathcal{V}_u$ and we assign this value to all the points belonging to it, $f_E(\boldsymbol{P}_f) = f_E(C_u)$ for all $\boldsymbol{P}_f \in \mathcal{V}_u$. Lastly, we save the value of this function in a look-up table, in which all the RULA indices are collected.

As a cobot, we employ the Racer5-0.80, an adaptable and flexible collaborative arm by the Italian corporation Comau [39]. The Denavit Hartenberg (DH) parameters and the dynamic parameters of the cobot are fed into the developed framework including the MATLAB Peter Corke Robotic Toolbox [40]. Table II shows the Racer5-0.80 DH characteristics, while Table III collects data related to mass (m), center of mass ($\boldsymbol{r}_{mi}$) of each link, and inertia matrices ($\boldsymbol{I}$). The motor inertia (J_m) and transmission ratio (G) of each link

TABLE II
DENAVIT HARTENBERG PARAMETERS FOR COMAU RACER5-0.80

Joint	q_i [rad]	d_i [m]	α_i [rad]	a_i [m]
Base	q_1	0.365	-1.571	0.05
Shoulder	q_2	0	0	0.37
Elbow	q_3	0	-1.571	0.05
Wrist 1	q_4	0.386	1.571	0
Wrist 2	q_5	0	-1.571	0
Wrist 3	q_6	0.08	0	0

are available on the manufacturer's website [39]. It should be noted that the center of mass is determined with respect to the i-th link reference frame, and link inertia matrices associated with the i-th link reference frame are calculated with good approximation by characterizing each link as a cylinder with different densities [41]. Additionally, the Racer5-0.80 base is set up in the workbench location $\boldsymbol{P}_w = (x_w, y_w, z_w)^\top = (0.15, -0.10, 1.00)^\top$ (coordinates in meters).

The starting and end points of the geometric rectilinear path are related to the orientation of the cobot's end-effector in Euler's angles (in radians) as follows: $\boldsymbol{\Phi}_i = (\phi_i, \theta_i, \psi_i)^\top = (1.396, 0.262, 2.007)^\top$ and $\boldsymbol{\Phi}_f = (\phi_f, \theta_f, \psi_f)^\top$ where $\phi_f = 1.396, \theta_f = 0.367, \psi_f = 1.571$ if $\boldsymbol{P}_f \in \{(P_{x_f}, P_{y_f}, P_{z_f})^\top \in \mathcal{V} | \, 0.2 \leq P_{x_f} \leq 0.5, -0.5 \leq P_{y_f} \leq 0.1, 1 \leq P_{z_f} < 1.437\}$, and $\phi_f = 1.571, \theta_f = 0, \psi_f = 1.222$ if $\boldsymbol{P}_f \in \{(P_{x_f}, P_{y_f}, P_{z_f})^\top \in \mathcal{V} | \, P_{z_f} \geq 1.435\}$.

Then, we select the parametric optimization function $\tilde{f}_T(\boldsymbol{P}_f)$, which is the function that identifies the traversal time to bring the work-piece from the starting point to each end point of the work volume. The value $\tilde{f}_T(\boldsymbol{P}_f)$ is the solution of the time-optimal trajectory planning problem (31).

In order to solve problem (31), a set of technical parameters must be carefully determined. For the speed (ineq. 18), and acceleration (ineq. 20) constraints, we specifically refer to the lower and upper Racer5-0.80 kinematic limits reported in Table IV, and to the torque limits (ineq. (16)) in [39]. The discretization interval Δs and parameter α are both equal to 0.1. Note that the end-effector's speed is limited by the values v obtained in the simulation through the SSM criterion.

Next, we solve the overall MOO control problem (32). Note that the mathematical formulation in (32) is nontrivial as it comprehends the minimization of two functions with different natures: $\tilde{f}_T$ in (31) is computed by solving the convex optimization problem formulated in (27), whereas f_E is calculated using the look-up table in which all the RULA indices are collected for each point of the work volume $\mathcal{V}$.

Due to the extremely non linear structure of the proposed optimization problem, we solve it employing a genetic algorithm. These solution algorithms are widely recognized as efficient and powerful global methods to handle non linear optimization problems [42]. In detail, we implement the problem in MATLAB using the *gamultiobj* function of the Global Optimization Toolbox with a tolerance parameter, i.e, *FunctionTolerance*, equal to 10^{-6}.

As regards the integration of the objective functions in the genetic algorithm, on the one hand, $f_E(\boldsymbol{P}_f)$ is computed with the built look-up table; on the other hand, for each point $\boldsymbol{P}_f \in \mathcal{V}$, $\tilde{f}_T(\boldsymbol{P}_f)$ is coded using the CVX Toolbox in MATLAB, an efficient solver for convex optimization problem in SOCP form [43], which is interfaced with the genetic algorithm.

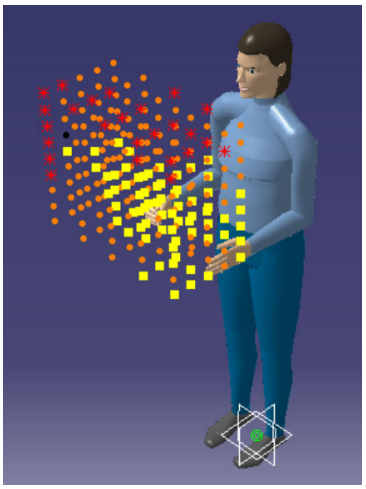

Fig. 4. Virtual manikin and work volume. We indicate the centroid C_u of each of these cuboids $\mathcal{V}_u$ with different shapes and colors: yellow squares (RULA 3), orange spots (RULA 4), and red stars (RULA 5).

B. Experimental Results

In order to evaluate the efficiency of the approach presented in this work, we analyze the results that are presented and discussed in detail in the current subsection.

The problem presented in Section III-D consists in finding an ergonomic point in the volume $\mathcal{V}$ (see Fig. 4), defined in Section III-A, that is the end point of the time-optimal trajectory taken by the end-effector of the Racer5-0.80.

As already mentioned in the previous sections, a RULA index is associated with the centroid of each sub-volume where ergonomics is assumed constant, as depicted in Fig. 4 with a color scale varying from yellow (for the minimum RULA index) passing through orange to red (for the highest RULA index). Hence, in our case study, the RULA index can have a score ranging from 3 (negligible risk) to 5 (medium risk that requires further investigation and must be changed soon) within volume $\mathcal{V}$.

As a result of the optimization problem (32), using the genetic algorithm (*gamultiobj*), we obtain three solutions on the Pareto front associated with the three RULA indices (Table V). It is clear from Table V that the two optimization goals are in competition with each other. The traversal time decreases together with the distance covered by the robot: indeed, the longest traversal time is associated with the lowest RULA index equal to 3, whereas the lowest time corresponds to the highest RULA index equal to 5. The smallest RULA region corresponds to points closer to the operator in the work volume $\mathcal{V}$ (Fig. 4), thus it is obvious that time is greater for these points. Therefore, the solution having a RULA index equal to 4 is a good trade-off between ergonomics and task efficiency. Nevertheless, we remark that the definitive choice of the end point of the robot's trajectory must be conducted by the decision maker. As mentioned above, the MOO problem is solved offline; thus, the computation time does not pose

TABLE III
DYNAMICS PARAMETERS FOR THE COMAU RACER5-0.80

Link	m [Kg]	$\boldsymbol{r}_{mi}$ [m]	$\boldsymbol{I}$ [kg m^2]
1	9.843	[0.002929, -0.000097, 0.153701]	[0.266 0 -0.005;0 0.285 0; -0.005 0 0.042]
2	5.131	[0.040000, -0.320000, -0.018000]	[0.564 0.069 0.004;0.069 0.038 -0.030; 0.004 -0.030 0.560]
3	8.242	[0.222000, -0.009000, -0.013000]	[0.235 0.029 0.029;0.029 0.432 -0.009; 0.029 -0.009 0.415]
4	3.320	[0.022000, -0.002000, 0.000300]	[0.008 0 -0.002;0 0.011 0; -0.002 0 0.008]
5	5.230	[-0.016000, 0.229000,-0.002000]	[0.316 0.002 0;0.002 0.009 0.002; 0 0.002 0.373]
6	0.979	[0, 0, 0.039000]	[0.002 0 0;0 0.002 0; 0 0 0]

TABLE IV
LOWER AND UPPER KINEMATIC LIMITS FOR THE COMAU RACER5-0.80

Link	q [rad]	$\dot{q}$ [rad/s]	$\ddot{q}$ [rad/s^2]
1	± 3.142	± 6.283	± 15.708
2	± 3.142	± 5.236	± 8.055
3	± 3.142	± 5.760	± 14.399
4	± 3.142	± 8.727	± 17.453
5	± 3.142	± 8.727	± 17.453
6	± 3.142	$\pm v$	± 27.890

TABLE V
SOLUTIONS OF THE MULTI-OBJECTIVE OPTIMIZATION PROBLEM

$\boldsymbol{P}_f$	Coordinates [m]	RULA	Time [s]
$\boldsymbol{P}_f^a$	[0.4250, −0.0500, 1.3125]	3	4.3847
$\boldsymbol{P}_f^b$	[0.3500, −0.3500, 1.4375]	4	1.7875
$\boldsymbol{P}_f^c$	[0.3500, −0.3500, 1.5000]	5	1.6964

a significant issue to consider for a practical application. In our setting, the computation time is approximately three hours, thus making the methodology implementable for any collaborative robotic system.

Uncertainty in robot components modeling and sensor measurements may result in a non-optimal positioning of the end-effector. This leads to a possible deviation from the optimum in the ergonomics and efficiency performance of the end point associated to the actually executed trajectory. Hence, it is important to evaluate the sensitivity of the results obtained by the MOO approach with respect to small spatial deviations of the end point from the optimum due to uncertainty. We analyze this effect by exploring two grids of 5×5 additional end points in the x-y and y-z planes centered in each of the above-mentioned Pareto frontier points as shown in Fig. 5. In particular, for each analyzed point, we represent the value of the RULA index with different colors (yellow, orange, and red for RULA equal to 3, 4, and 5, respectively), whilst the traversal time is denoted in accordance with a blue colormap (the higher the time, the higher the color intensity). From the figure, it is clear that the points with a RULA index equal to 5 (which have a lower traversal time than the former ones, as expected) do not show significant variation in the traversal time. Conversely, by analyzing both the points with a RULA index equal to 3 and the ones with a RULA index equal to 4, it is interesting to note that the traversal time has a non negligible variation, even if the spatial deviation of the end point is small, and this effect could thus be taken into account as a criterion in the choice of the Pareto solution.

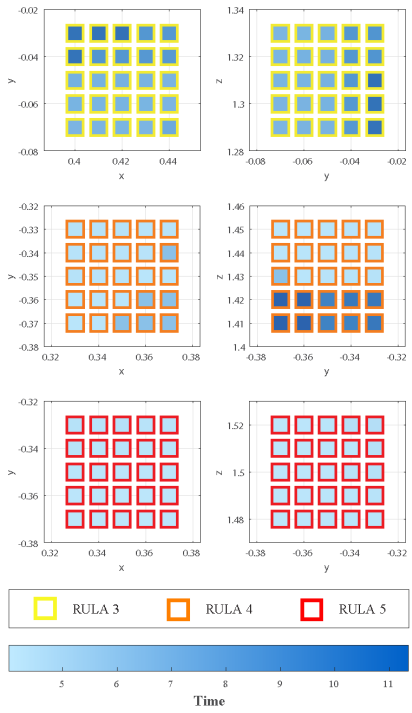

Fig. 5. Results of the sensitivity analysis on Pareto solutions obtained by the proposed method: the plots show the variation of the RULA index and traversal time induced by moving the end-effector position in the x-y and y-z planes. For the analyzed end points, the RULA index is represented by different edge colors (yellow, orange, and red for RULA equal to 3, 4, and 5, respectively), whilst the traversal time is denoted in accordance with a blue colormap (higher the time, higher the color intensity).

V. CONCLUSION

Trajectory planning is one of the major challenges addressed in the robotics and cobotics literature. Indeed, speeding up a task in real experiments and/or industrial applications, can increase profitability for industrial players.

In this paper, we propose a novel multi-objective optimization approach for time-optimal trajectory planning in a safe and ergonomic HRC scenario with the aim of guaranteeing the best compromise between ergonomics for the human worker and time efficiency for the cobot, while adhering to the Speed and Separation Monitoring ISO safety regulations. The effectiveness of the proposed technique is verified through an experimental case study on the Comau Racer5-0.80, while the manikin replicating the operator is developed in the CATIA software and the optimization problem is solved by a genetic algorithm in the MATLAB environment.

Future works will focus on enhancing the safe and ergonomic HRC architecture by accounting for unpredictable

human behaviors and thus by replanning online the trajectory taking into account large variations in the position and eventually physical features of the operators that collaborate with the robot. In this perspective, our proposed technique should be extended and integrated with other ad-hoc methodologies. For instance, a future development could consist in the offline definition, with the proposed approach, of a proper database of trajectories that considers the most varied positions of several types of operators with different characteristics (i.e., gender, height, weight). The database could provide the appropriate trajectory and control actions depending on the considered scenario (i.e., the features of the operator and the monitored and/or predicted dynamics of the operator). Finally, it may be convenient to evaluate the RULA index on a more advanced manikin that is able to emulate reality more accurately.

ACKNOWLEDGMENT

The authors would like to thank the Comau S.p.A.—Technology Office, particularly the Head of Cognitive Robotics Simone Panicucci, the Head of Automation Systems Nicola Longo, and the Software Technologies Engineer Luca Di Ruscio, for their precious support in the preparation of this article.

REFERENCES

[1] A. Cardoso, A. Colim, E. Bicho, A. C. Braga, M. Menozzi, and P. Arezes, "Ergonomics and human factors as a requirement to implement safer collaborative robotic workstations: A literature review," *Safety*, vol. 7, no. 4, p. 71, Oct. 2021.

[2] H. Li, X. Wang, X. Huang, Y. Ma, and Z. Jiang, "Multi-joint active collision avoidance for robot based on depth visual perception," *IEEE/CAA J. Autom. Sinica*, vol. 9, no. 12, pp. 2186–2189, Dec. 2022.

[3] X. Ren, Z. Li, M. Zhou, and Y. Hu, "Human intention-aware motion planning and adaptive fuzzy control for a collaborative robot with flexible joints," *IEEE Trans. Fuzzy Syst.*, vol. 31, no. 7, pp. 2375–2388, Jul. 2023.

[4] S. Proia, G. Cavone, A. Camposeo, F. Ceglie, R. Carli, and M. Dotoli, "Safe and ergonomic human-drone interaction in warehouses," in *Proc. IEEE/RSJ Int. Conf. Intell. Robots Syst. (IROS)*, Oct. 2022, pp. 6681–6686.

[5] L. McAtamney and E. N. Corlett, "RULA: A survey method for the investigation of work-related upper limb disorders," *Appl. Ergonom.*, vol. 24, no. 2, pp. 91–99, Apr. 1993.

[6] V. M. Manghisi, A. E. Uva, M. Fiorentino, V. Bevilacqua, G. F. Trotta, and G. Monno, "Real time RULA assessment using Kinect v2 sensor," *Appl. Ergonom.*, vol. 65, pp. 481–491, Nov. 2017.

[7] A. M. Zanchettin, E. Lotano, and P. Rocco, "Collaborative robot assistant for the ergonomic manipulation of cumbersome objects," in *Proc. IEEE/RSJ Int. Conf. Intell. Robots Syst. (IROS)*, Nov. 2019, pp. 6729–6734.

[8] S. Proia, R. Carli, G. Cavone, and M. Dotoli, "A literature review on control techniques for collaborative robotics in industrial applications," in *Proc. IEEE 17th Int. Conf. Autom. Sci. Eng. (CASE)*, Aug. 2021, pp. 591–596.

[9] S. Proia, R. Carli, G. Cavone, and M. Dotoli, "Control techniques for safe, ergonomic, and efficient human–robot collaboration in the digital industry: A survey," *IEEE Trans. Autom. Sci. Eng.*, vol. 19, no. 3, pp. 1798–1819, Jul. 2022.

[10] A. Palleschi et al., "Time-optimal trajectory planning for flexible joint robots," *IEEE Robot. Autom. Lett.*, vol. 5, no. 2, pp. 938–945, Apr. 2020.

[11] K. Shin and N. McKay, "Minimum-time control of robotic manipulators with geometric path constraints," *IEEE Trans. Autom. Control*, vol. 30, no. 6, pp. 531–541, Jun. 1985.

[12] J. E. Bobrow, S. Dubowsky, and J. S. Gibson, "Time-optimal control of robotic manipulators along specified paths," *Int. J. Robot. Res.*, vol. 4, no. 3, pp. 3–17, Sep. 1985.

[13] K. Shin and N. McKay, "A dynamic programming approach to trajectory planning of robotic manipulators," *IEEE Trans. Autom. Control*, vol. 31, no. 6, pp. 491–500, Jun. 1986.

[14] S. Singh and M. C. Leu, "Optimal trajectory generation for robotic manipulators using dynamic programming," *J. Dyn. Syst., Meas., Control*, vol. 109, no. 2, pp. 88–96, Jun. 1987.

[15] J. T. Betts and W. P. Huffman, "Path-constrained trajectory optimization using sparse sequential quadratic programming," *J. Guid., Control, Dyn.*, vol. 16, no. 1, pp. 59–68, Jan. 1993.

[16] D. Constantinescu and E. A. Croft, "Smooth and time-optimal trajectory planning for industrial manipulators along specified paths," *J. Robot. Syst.*, vol. 17, no. 5, pp. 233–249, May 2000.

[17] P. R. Mora, *On the Time-Optimal Trajectory Planning Along Predetermined Geometric Paths and Optimal Control Synthesis for Trajectory Tracking of Robot Manipulators*. Berkeley, CA, USA: Univ. of Berkeley, 2013.

[18] D. Verscheure, B. Demeulenaere, J. Swevers, J. De Schutter, and M. Diehl, "Time-optimal path tracking for robots: A convex optimization approach," *IEEE Trans. Autom. Control*, vol. 54, no. 10, pp. 2318–2327, 2009.

[19] A. Palleschi, M. Hamad, S. Abdolshah, M. Garabini, S. Haddadin, and L. Pallottino, "Fast and safe trajectory planning: Solving the cobot performance/safety trade-off in human–robot shared environments," *IEEE Robot. Autom. Lett.*, vol. 6, no. 3, pp. 5445–5452, Jul. 2021.

[20] F. Ferraguti, R. Villa, C. T. Landi, A. M. Zanchettin, P. Rocco, and C. Secchi, "A unified architecture for physical and ergonomic human–robot collaboration," *Robotica*, vol. 38, no. 4, pp. 669–683, Apr. 2020.

[21] L. Gualtieri, E. Rauch, and R. Vidoni, "Emerging research fields in safety and ergonomics in industrial collaborative robotics: A systematic literature review," *Robot. Comput.-Integr. Manuf.*, vol. 67, Feb. 2021, Art. no. 101998.

[22] A. Hentout, M. Aouache, A. Maoudj, and I. Akli, "Human–robot interaction in industrial collaborative robotics: A literature review of the decade 2008–2017," *Adv. Robot.*, vol. 33, nos. 15–16, pp. 764–799, Aug. 2019.

[23] G. Tresca, G. Cavone, R. Carli, A. Cerviotti, and M. Dotoli, "Automating bin packing: A layer building matheuristics for cost effective logistics," *IEEE Trans. Autom. Sci. Eng.*, vol. 19, no. 3, pp. 1599–1613, Jul. 2022.

[24] G. Cavone, A. Bozza, R. Carli, and M. Dotoli, "MPC-based process control of deep drawing: An industry 4.0 case study in automotive," *IEEE Trans. Autom. Sci. Eng.*, vol. 19, no. 3, pp. 1586–1598, Jul. 2022.

[25] S. Proia, G. Cavone, R. Carli, and M. Dotoli, "A multi-objective optimization approach for trajectory planning in a safe and ergonomic human–robot collaboration," in *Proc. IEEE 18th Int. Conf. Autom. Sci. Eng. (CASE)*, Aug. 2022, pp. 2068–2073.

[26] *Robots and Robotic Devices—Collaborative Robots*, Standard ISO/TS 15066, International Organization for Standardization, 2016.

[27] D. Colombini, A. Grieco, and E. Occhipinti, "Occupational musculoskeletal disorders of the upper limbs due to mechanical overload," *Ergonomics*, vol. 41, no. 9, 1998.

[28] Nikhilkumar, S. M. Qutubuddin, R. P. Pallavi, A. Sambrani, and D. Padashetty, "Analysis of working postures in a small-scale fastener industry by rapid upper limb assessment (RULA) using CATIA software," in *Technology Enabled Ergonomic Design*. Singapore: Springer, 2022, pp. 75–85.

[29] S. Baskaran et al., "Digital human and robot simulation in automotive assembly using Siemens process simulate: A feasibility study," *Proc. Manuf.*, vol. 34, pp. 986–994, Jan. 2019.

[30] C. Byner, B. Matthias, and H. Ding, "Dynamic speed and separation monitoring for collaborative robot applications—Concepts and performance," *Robot. Comput.-Integr. Manuf.*, vol. 58, pp. 239–252, Aug. 2019.

[31] N. Lucci, B. Lacevic, A. M. Zanchettin, and P. Rocco, "Combining speed and separation monitoring with power and force limiting for safe collaborative robotics applications," *IEEE Robot. Autom. Lett.*, vol. 5, no. 4, pp. 6121–6128, Oct. 2020.

[32] J. A. Marvel and R. Norcross, "Implementing speed and separation monitoring in collaborative robot workcells," *Robot. Comput.-Integr. Manuf.*, vol. 44, pp. 144–155, Apr. 2017.

[33] G. Belingardi, S. Heydaryan, and P. Chiabert, "Application of speed and separation monitoring method in human–robot collaboration: Industrial case study," in *Proc. 17th Int. Sci. Conf. Ind. Syst.*, 2017, pp. 96–101.

[34] S. Boyd and L. Vandenberghe, *Convex Optimization*. Cambridge, U.K.: Cambridge Univ. Press, 2004.

[35] Z. Zhao, S. Liu, M. Zhou, and A. Abusorrah, "Dual-objective mixed integer linear program and memetic algorithm for an industrial group scheduling problem," *IEEE/CAA J. Autom. Sinica*, vol. 8, no. 6, pp. 1199–1209, Jun. 2021.

[36] H. Li, B. Wang, Y. Yuan, M. Zhou, Y. Fan, and Y. Xia, "Scoring and dynamic hierarchy-based NSGA-II for multiobjective workflow scheduling in the cloud," *IEEE Trans. Autom. Sci. Eng.*, vol. 19, no. 2, pp. 982–993, Apr. 2022.

[37] Z. Ning et al., "Online scheduling and route planning for shared buses in urban traffic networks," *IEEE Trans. Intell. Transp. Syst.*, vol. 23, no. 4, pp. 3430–3444, Apr. 2022.

[38] X. Guo et al., "Human–robot collaborative disassembly line balancing problem with stochastic operation time and a solution via multi-objective shuffled frog leaping algorithm," *IEEE Trans. Autom. Sci. Eng.*, early access, Jul. 28, 2023, doi: 10.1109/TASE.2023.3296733.

[39] *Comau Website*. Accessed: Apr. 1, 2021. [Online]. Available: https://www.comau.com/it/competencies/robotics-automation/collaborative-robotics/racer-5-0-80-cobot/

[40] *Peter Corke Toolbox Website*. Accessed: Dec. 1, 2021. [Online]. Available: https://petercorke.com/toolboxes/robo-tics-toolbox/

[41] K. Kufieta, "Force estimation in robotic manipulators: Modeling," M.S. thesis, NTNU Norwegian Univ. Sci. Technol., 2014. [Online]. Available: https://folk.ntnu.no/tomgra/Diplomer/Kufieta.pdf

[42] K. Gallagher and M. Sambridge, "Genetic algorithms: A powerful tool for large-scale nonlinear optimization problems," *Comput. Geosci.*, vol. 20, nos. 7–8, pp. 1229–1236, Aug. 1994.

[43] *CVX Toolbox Website*. Accessed: Dec. 1, 2021. [Online]. Available: http://cvxr.com/cvx/

Silvia Proia (Member, IEEE) received the double M.Sc. degree in mechanical engineering with major in mechatronics and robotics from the Polytechnic University of Bari, Italy, and NYU Tandon School of Engineering, USA, in 2020, where she is currently pursuing the Ph.D. degree with the Electrical and Information Engineering Department, advised by Prof. Ing. Mariagrazia Dotoli.

During the M.Sc. degree, she worked on biomedical devices, telerobotics systems, signal processing and on electromyography, and an innovative method to control prostheses. Her research interests include industry 4.0, automation, decision, and control techniques for collaborative robotic systems.

Graziana Cavone (Senior Member, IEEE) received the master's degree (summa cum laude) in control engineering from the Polytechnic of Bari, Italy, in 2013, and the Ph.D. degree (Hons.) in electronic and computer engineering from the University of Cagliari, Italy, in 2018.

She is currently an Assistant Professor in automatic control with Roma Tre University. From 2018 to 2022, she was a Post-Doctoral Research Fellow with the Polytechnic of Bari, and a Visiting Ph.D. Student with the Delft University of Technology, The Netherlands, from 2016 to 2017. Her research interests include the definition, simulation, and application of decision and control techniques to discrete-event and hybrid systems, manufacturing systems, railway networks, logistics, energy systems, and smart cities. She is the Diversity and Inclusion Co-Chair for the International Conference on Automation Science and Engineering 2024. She was the Local Arrangements Chair of the 2021 Mediterranean Conference on Control and Automation. She is an Associate Editor of the *International Journal Results in Control and Optimization* (RICO). She was a member of the International Program Committee of more than 30 international conferences and a Guest Editor for special issues on international journals. She was awarded a research grant by the National Science Foundation of China for year 2020. She is author of more than 50 printed international publications.

Paolo Scarabaggio (Member, IEEE) received the B.Sc. degree in mechanical engineering and the M.Sc. degree in management engineering from Politecnico di Bari, Bari, Italy, in 2017 and 2019, respectively, where he is currently pursuing the Ph.D. degree with the Department of Electrical and Information Engineering under the supervision of Prof. Engr. Mariagrazia Dotoli.

In 2019, he was a Visiting Student with the Delft Center for Systems and Control, TU Delft, The Netherlands. His research interests include the modeling, optimization, and distributed control of energy and complex networked systems.

Raffaele Carli (Senior Member, IEEE) received the Laurea degree (Hons.) in electronic engineering and the Ph.D. degree in electrical and information engineering from Politecnico di Bari, Italy, in 2002 and 2016, respectively.

From 2003 to 2004, he was a Reserve Officer with Italian Navy. From 2004 to 2012, he was a System and Control Engineer and the Technical Manager for a space and defense multinational company. He is currently an Assistant Professor in automatic control with Politecnico di Bari. His research interests include the formalization, simulation, and implementation of decision and control systems, and the modeling and optimization of complex systems.

Dr. Carli is an Associate Editor of IEEE TRANSACTIONS ON AUTOMATION SCIENCE AND ENGINEERING and IEEE TRANSACTIONS ON SYSTEMS, MAN, AND CYBERNETICS. He was a member of the International Program Committee of more than 30 international conferences and a guest editor for special issues in international journals. He is the author of more than 80 printed international publications.

Mariagrazia Dotoli (Senior Member, IEEE) received the Laurea degree (Hons.) in electronic engineering and the Ph.D. degree in electrical engineering from Politecnico di Bari, Italy, in 1995 and 1999, respectively.

She has been a Visiting Scholar with the Paris 6 University and the Technical University of Denmark. She is an Expert Evaluator of the European Commission since the Sixth Framework Program. She is currently a Full Professor in automatic control with Politecnico di Bari, where she joined in 1999. She has been the Vice Rector for Research of Politecnico di Bari and a Member Elect of the Academic Senate. Her research interests include the modeling, identification, management, control and diagnosis of discrete event systems, manufacturing systems, logistics systems, traffic networks, smart grids, and networked systems.

Prof. Dotoli was the Co-Chairperson of the Training and Education Committee of ERUDIT, the European Commission network of excellence for fuzzy logic and uncertainty modeling in information technology, and she was a Key Node Representative of EUNITE, the EUropean Network of Excellence on Intelligent Technologies. She is a Senior Editor of IEEE TRANSACTIONS ON AUTOMATION SCIENCE AND ENGINEERING and an Associate Editor of IEEE TRANSACTIONS ON SYSTEMS, MAN, AND CYBERNETICS. She is the General Chair of the 2024 IEEE Conference on Automation Science and Engineering. She was the General Chair of the 2021 Mediterranean Conference on Control and Automation, the Program Chair of the 2020 IEEE Conference on Automation Science and Engineering, the Program Co-Chair of the 2017 IEEE Conference on Automation Science and Engineering, the Workshop and Tutorial Chair of the 2015 IEEE Conference on Automation Science and Engineering, the Special Session Co-Chair of the 2013 IEEE Conference on Emerging Technology and Factory Automation, and the Chair of the National Committee of the 2009 IFAC Workshop on Dependable Control of Discrete Systems. She was a member of the International Program Committee of more than 80 international conferences. She is the author of more than 200 publications, including one textbook (in Italian) and more than 70 international journal articles.

Open Access funding provided by 'Politecnico di Bari' within the CRUI CARE Agreement